



Share Your Innovations through JACS Directory

Journal of Nanoscience and Technology

Visit Journal at <https://www.jacsdirectory.com/jnst>

Structural Analysis of the Indium Substituted Ni-Cu-Zn Ferrites using XRD Technique

Mohsin Y. Shaha^{1,*}, Mahendra M. Bagul¹, Ajay A. Nikam¹, Nandkishor D. Chaudhari²¹Department of Electronics, MVP Samaj's Arts, Commerce and Science College, Dindori, Nashik – 422 202, Maharashtra, India.²Departments of Physics, Pratishthan Mahavidyalaya Paithan, Sambhajinagar – 431 107, Maharashtra, India.

ARTICLE DETAILS

Article history:

Received 24 February 2026

Accepted 11 March 2026

Available online 15 April 2026

Keywords:

Nickel-Copper-Zinc Ferrite

X-Ray Powder Diffraction

Sol-Gel Auto-Combustion Technique

ABSTRACT

Nickel-copper-zinc ferrite samples, $\text{Ni}_{0.35}\text{Cu}_{0.05}\text{Zn}_{0.60}\text{In}_x\text{Fe}_{2-x}\text{O}_4$, with $x = 0.00$ to $x = 0.125$ were prepared by sol-gel auto combustion method. The chemical phase analysis has been carried out by X-ray powder diffraction (XRD) method, which confirms the formation single phased cubic spinel structure with a crystallite size ranging from 25 to 45 nm. While increasing indium concentration, the lattice constant increases. On the XRD plot, this causes the diffraction peaks to shift toward lower 2θ angles. Since indium has a much higher atomic weight than iron, the X-ray density calculated from the XRD data will increase significantly as indium replaces iron. A higher peak intensity for indium-doped samples usually suggests improved crystallinity.

1. Introduction

Ferrite materials of spinel structural formula AB_2O_4 are mainly composed of about 70% iron oxide (Fe_2O_3) and about 30% of other metal oxides including MgO, MnO, NiO, CuO, etc., [1]. Each spinel unit cell contains eight formula units. In each unit cell, there are 64 tetrahedral sites (A sites) and 32 octahedral sites (B sites) [2]. On the basis of distribution of metal ions at (A) and (B) site, spinel ferrites are of three types; namely normal, inverse and random spinel ferrite. The high electrical resistivity, low eddy current and dielectric loss, high saturation magnetization, high permeability, good chemical stability, ease of preparation, low cost of production etc., are the remarkable features of spinel ferrites. Magnetic spinel nano ferrites have attracted the interest of the researchers due to their importance in understanding the fundamentals of nano magnetism and their wide range of applications. They found potential applications in bio- medicine such as magnetic resonance imaging (MRI), targeted drug delivery, magnetic separation [3]. NiCuZn ferrites are excellent soft magnetic materials in high frequency device due to their low cost, high resistivity and low eddy current losses that have been extensively studied for multi-layer chip inductor (MLCI) applications [4]. Extensive research has investigated how various dopants influence the Ni-Cu-Zn ferrite matrix, specifically aiming to improve its dielectric, magnetic, and structural parameters for advanced applications. Over the past few decades, research has pivoted toward developing innovative techniques to enhance the structural and magnetic characteristics of soft magnetic spinel ferrites [5]. Specifically, Ni-Cu-Zn ferrites have garnered significant attention due to their critical role in the fabrication of multilayer chip inductors (MLCIs). While various synthesis strategies—ranging from traditional solid-state ceramic methods to sol-gel self-propagation—have been employed, the sol-gel auto-combustion route stands out [6]. This method is increasingly preferred for its ability to produce highly stoichiometric, nano-scaled powders at reduced processing temperatures and lower operational costs [7].

This present work focus on the synthesis of NiCuZn ferrite powders by a solgel auto-combustion technique. This is a novel way with a unique combination of the chemical solgel process and the combustion process. The process has the advantages of inexpensive precursors, a simple preparation method, and a resulting nano-sized, homogeneous, highly reactive powder [8]. Also, the work is discussing about X-ray powder diffraction (XRD) method, formation of single phased cubic spinel structure, crystallite size, the lattice constant and X-ray density.

2. Experimental Methods

For the synthesis of nanocrystalline $\text{Ni}_{0.35}\text{Cu}_{0.05}\text{Zn}_{0.60}\text{In}_x\text{Fe}_{2-x}\text{O}_4$ ferrites (where $x = 0.0$ to 0.125 in increments of 0.025) high-purity (99.9%) precursors were utilized via the citrate-nitrate auto-combustion technique. The metal nitrates specifically nickel nitrate ($\text{Ni}(\text{NO}_3)_2 \cdot 6\text{H}_2\text{O}$), copper nitrate ($\text{Cu}(\text{NO}_3)_2 \cdot 6\text{H}_2\text{O}$), zinc nitrate ($\text{Zn}(\text{NO}_3)_2 \cdot 6\text{H}_2\text{O}$), indium nitrate ($\text{In}(\text{NO}_3)_3 \cdot 9\text{H}_2\text{O}$), and ferric nitrate ($\text{Fe}(\text{NO}_3)_3 \cdot 9\text{H}_2\text{O}$) served as the primary reactants, while citric acid monohydrate $\text{C}_6\text{H}_8\text{O}_7 \cdot \text{H}_2\text{O}$ acted as the fuel and chelating agent.

Aqueous solutions of metal nitrates and citric acid were combined, maintaining a stoichiometric 1:3 molar ratio. The resulting mixture was subjected to continuous agitation via a magnetic stirrer to ensure the formation of a uniform citrate-nitrate precursor solution [9]. The precursor solution was evaporated through heating until a gel phase was established. This gel was subsequently dehydrated in an air oven at 100°C to eliminate residual moisture. During dehydration, the material expanded into a voluminous, fluffy mass before fragmenting into brittle flakes. The resulting precursor was calcined at 600°C for 4 h to yield the nanocrystalline ferrites. A comprehensive schematic of the synthesis and characterization workflow is presented in Fig. 1.

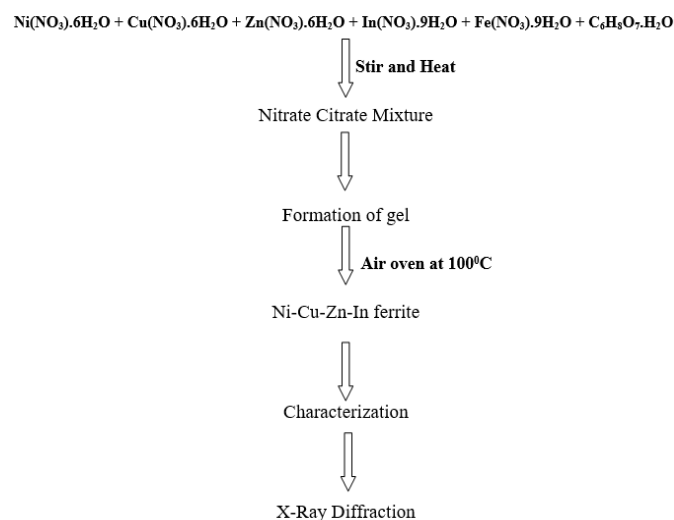


Fig. 1 Flowchart for the synthesis and characterization of Ni-Cu-Zn-In Nano ferrites

*Corresponding Author: princemosin@gmail.com (Mohsin Y. Shaha)



Phase identification and the verification of chemical reaction completion were conducted using X-ray diffraction (XRD). Patterns were recorded on a Rigaku D/MAX-IIA diffractometer utilizing $\text{CuK}\alpha$ radiation. Data collection was performed over a 2θ range of $20\text{--}70^\circ$ with a constant scanning rate of 2.9×10^{-4} rad/s. The lattice parameters and X-ray densities of the samples were calculated from the diffraction pattern (Fig. 1) [10]. The sintered density was determined from the mass and bulk volume of the samples. By comparing the values of both densities, the porosity for each sample was determined.

3. Results and Discussion

Fig. 2 illustrates the XRD pattern of developed indium substituted NiCuZn ferrite samples with $x = 0.00 - 0.125$ for the general composition $\text{Ni}_{0.35}\text{Cu}_{0.05}\text{Zn}_{0.60}\text{In}_x\text{Fe}_{2-x}\text{O}_4$. The XRD spectra showed the crystallite state of ferrites that possess cubic spinel structure. The obtained planes (220), (311), (222), (400), (422), (511) and (440) confirmed the formation of cubic spinel structure having $\text{Fd}3\text{m}$ space group. No any further impurity peaks are obtained in the XRD, which clearly specifies the developed material is of good quality in terms of purity [11].

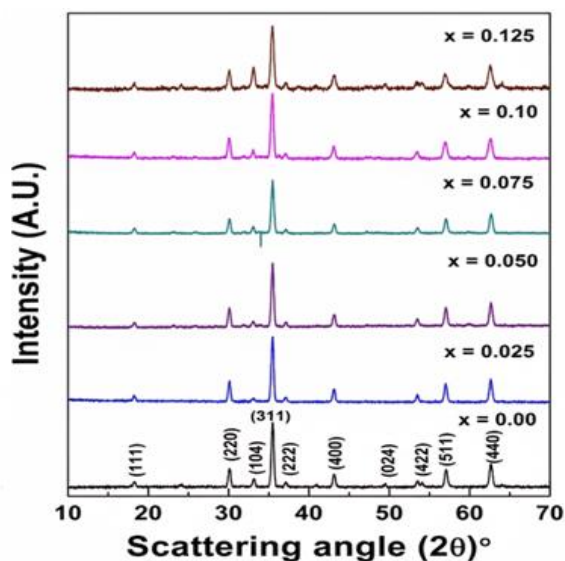


Fig. 2 XRD pattern of developed indium substituted NiCuZn ferrite samples

Sol-gel auto combustion method is a bottom-up chemical route the resulting powder is nanocrystalline the XRD report will typically include, crystalline size (D) calculated using the Scherrer formula, typically ranges from 25 nm to 45 nm. The X-ray density (ρ_x) usually increases because the atomic weight of indium (114.82 u) is much higher than that of iron (55.84 u) [12]. Effect of indium on lattice parameters as Indium In^{3+} has a larger ionic radius 0.80 \AA than Iron (Fe^{3+}) 0.645 \AA as a result the XRD report will show, peak shifts towards lower 2θ angles as indium concentration

increases, there is linear increase in lattice parameter, the cell volume also increases [13].

4. Conclusion

This study demonstrates that the sol-gel auto-combustion technique is an effective route for producing high-purity In^{3+} substituted NiCuZn ferrites. Structural characterization via XRD verified that all samples maintained a cubic spinel phase without impurity formation. As the substitution of Indium ions was achieved without disrupting the lattice integrity, the increase in Indium concentration x factors the formation of NiCuZn ferrites with higher density. X-ray density depends on the lattice constant and molecular weight of the samples shows an increasing trend with increasing Indium content. These nano-ferrites show significant potential for miniaturized magnetic components. The high homogeneity and refined particle size achieved at a relatively low calcination temperature (600°C) highlight the advantages of this processing approach.

References

- [1] D.J. Sellmyer, C.P. Luo, Y. Qiang, J.P. Liu, Magnetic nanocomposites, in: D.J. Sellmyer, R. Skomski (Eds.), Handbook of thin films, Academic Press, Burlington, 2002, pp.337–374.
- [2] R.P. Patil, S.D. Delekar, D.R. Mane, P.P. Hankare, Synthesis, structural and magnetic properties of different metal ion substituted nanocrystalline zinc ferrite, Results Phys. 3 (2013) 129–133.
- [3] S. Laurent, D. Forge, M. Port, A. Roch, C. Robic, et al., Magnetic iron oxide nanoparticles: synthesis, vectorization, physico-chemical characterizations and biological applications, Chem. Rev. 108 (2008) 2064–2110.
- [4] S. Mornet, S. Vasseur, F. Grasset, E. Duguet, Magnetic nanoparticle design for medical diagnosis and therapy, J. Mater. Chem. 14 (2004) 2161–2164.
- [5] T. Matsunaga, Y. Okamura, T. Tanaka, Biotechnological application of nano-scale engineered bacterial magnetic particles, J. Mater. Chem. 14 (2004) 2099–2105.
- [6] S.E. Shirsath, R.H. Kadam, S.M. Patange, M.L. Mane, A. Ghasemi, et al., Enhanced magnetic properties of Dy^{3+} substituted Ni–Cu–Zn ferrite nanoparticles, Appl. Phys. Lett. 100 (2012) 042407.
- [7] P.K. Roy, J. Bera, Effect of Mg substitution on electromagnetic properties of $(\text{Ni}_{0.25}\text{Cu}_{0.20}\text{Zn}_{0.55})\text{Fe}_2\text{O}_4$ ferrite prepared by auto combustion method, J. Magn. Magn. Mater. 298 (2006) 38–42.
- [8] P.A. Jadhav, R.S. Devan, Y.D. Kolekar, B.K. Chougule, Structural, electrical and magnetic characterizations of Ni–Cu–Zn ferrite synthesized by citrate precursor method, J. Phys. Chem. Solids 70 (2009) 396–400.
- [9] A.A. Sattar, Physical, magnetic and electrical properties of Ga substituted Mn ferrites, Egypt. J. Solids 27 (2004) 99–110.
- [10] J. Schäfer, W. Sigmund, S. Roy, F. Aldinger, Low temperature synthesis of ultrafine $\text{Pb}(\text{Zr},\text{Ti})\text{O}_3$ powder by sol-gel combustion, J. Mater. Res. 12 (1997) 2518–2521.
- [11] A. Chakraborty, P. Sujatha Devi, H.S. Maiti, Preparation of $\text{La}_{1-x}\text{Sr}_x\text{MnO}_3$ ($0 < x < 0.6$) powder by auto-ignition of carboxylate–nitrate gels, Mater. Lett. 20 (1994) 63–66.
- [12] Y.K. Sun, I.H. Ahn, S.A. Hong, Synthesis of ultrafine LiCoO_2 powders by the sol-gel method, J. Mater. Sci. 31 (1996) 3617–3620.
- [13] N. Chakrabarti, H.S. Maiti, Chemical synthesis of PZT powder by auto-combustion of citrate–nitrate gel, Mater. Lett. 30 (1997) 169–173.

Special Issue Publication Statement

This article is included in the Special Issue of the journal comprising peer-reviewed papers selected from the International Conference on “Frontiers in Chemical and Material Sciences (ICFCMS-2026)”, held on 3rd and 4th February 2026 at MGV’s Maharaja Sayajirao Gaikwad Arts, Science and Commerce College, Malegaon Camp, Malegaon, Nashik – 423 105, Maharashtra, India.